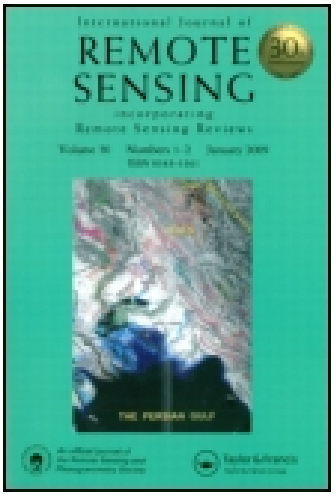


International Journal of Remote Sensing

Publication details, including instructions for authors and subscription information:
http://www.tandfonline.com/loi/tres20

# Surface and total ozone investigations in the region of Sofia, Bulgaria

Vera Grigorieva [a], Nikolay Kolev [a], Evgeni Donev [b], Danko Ivanov [b], Bogdana Mendeva [c], Tsvetina Evgenieva [a], Vladislav Danchovski [b] & Ivan Kolev [a]

[a] Institute of Electronics, Bulgarian Academy of Sciences, 1784, Sofia, Bulgaria

[b] Department of Meteorology and Geophysics, Faculty of Physics, Sofia University 'St Kliment Ohridsky', 1164, Sofia, Bulgaria

[c] Solar-Terrestrial Influences Laboratory, Bulgarian Academy of Sciences, 1113, Sofia, Bulgaria

Published online: 24 Nov 2011.

To cite this article: Vera Grigorieva, Nikolay Kolev, Evgeni Donev, Danko Ivanov, Bogdana Mendeva, Tsvetina Evgenieva, Vladislav Danchovski & Ivan Kolev (2012) Surface and total ozone investigations in the region of Sofia, Bulgaria, International Journal of Remote Sensing, 33:11, 3542-3556, DOI: 10.1080/01431161.2011.621904

To link to this article: http://dx.doi.org/10.1080/01431161.2011.621904

*International Journal of Remote Sensing*
Vol. 33, No. 11, 10 June 2012, 3542–3556

Taylor & Francis
Taylor & Francis Group

# Surface and total ozone investigations in the region of Sofia, Bulgaria

VERA GRIGORIEVA*†, NIKOLAY KOLEV†, EVGENI DONEV‡, DANKO IVANOV‡, BOGDANA MENDEVA§, TSVETINA EVGENIEVA†, VLADISLAV DANCHOVSKI‡ and IVAN KOLEV†

†Institute of Electronics, Bulgarian Academy of Sciences, 1784 Sofia, Bulgaria
‡Department of Meteorology and Geophysics, Faculty of Physics, Sofia University 'St Kliment Ohridsky', 1164 Sofia, Bulgaria
§Solar-Terrestrial Influences Laboratory, Bulgarian Academy of Sciences, 1113 Sofia, Bulgaria

(*Received 31 November 2009; in final form 7 July 2011*)

Atmospheric ozone behaviour over Sofia has been investigated with remote-sensing and *in situ* techniques. Surface ozone and boundary layer observations performed in recent years at three city sites have been analysed. It was found that, in the autumn period, at close meteorological conditions, diurnal ozone variations show stable behaviour from year to year during the analysed period. It may be assumed that the boundary layer and ozone precursor concentrations, which are involved in photochemical ozone formation, keep up their state from year to year at the mentioned conditions. These findings may be interesting when surface ozone trends and climate change influence on ozone are investigated. The analysis of the long-term total ozone content (TOC) variations did not find a total ozone trend in the 1997–2008 period.



## 1. Introduction

The dynamics of atmospheric ozone, which is one of the factors affecting the Earth's climate, is closely studied on global (Reid *et al.* 1994, Gernandt *et al.* 1995, Reid *et al.* 1998, Efstathiou *et al.* 2003, Varotsos *et al.* 2004), regional (Varotsos and Cracknell 1993, Chandra and Varotsos 1995, Schulz *et al.* 2000, 2001) and local (Kondratyev *et al.* 1994, Varotsos and Cracknell 1994, Varotsos *et al.* 2000) scales.

Ozone actively takes part in different processes, which implement interactions in the complex sun–atmosphere–Earth–human activity system (Kondratyev and Varotsos 1995a,b, Varotsos and Cracknell 2004, Bandyopadhyay and Chattopadhyay 2007, Chattopadhyay and Bandyopadhyay 2007). Depletion of the ozone layer leads to an increase in the ultraviolet radiation that penetrates onto the Earth's surface (Varotsos 1994, Kondratyev *et al.* 1995, Varotsos *et al.* 1995, Kondratyev and Varotsos 1996, Efstathiou *et al.* 1998, Ziemke *et al.* 2000, Varotsos *et al.* 2001a). Having relatively strong absorption within the vibration–rotation band near 9.6 μm, ozone absorbs terrestrial infrared radiation, strengthening the greenhouse effect and, together with the main greenhouse gases ($H_2O$, $CO_2$, $CH_4$), causes warming of the Earth's atmosphere and surface. The primary evidence of this effect are the temperature and increasing moisture. In the lower troposphere, ozone is mostly of anthropogenic origin. It is a

*Corresponding author. Email: veragrigorieva@gmail.com; grig@ie.bas.bg

*International Journal of Remote Sensing*
ISSN 0143-1161 print/ISSN 1366-5901 online © 2012 Taylor & Francis
http://www.tandf.co.uk/journals
http://dx.doi.org/10.1080/01431161.2011.621904

secondary pollutant, which is formed as a result of complex photochemical reactions induced by solar radiation with participation of $O_3$ precursors – nitrogen oxides $NO_X$ ($NO_X$: $NO + NO_2$) and volatile organic components (VOCs) (Cartalis and Varotsos 1994, Jacovides *et al.* 1994, Varotsos *et al.* 2001b, Kondratyev and Varotsos 2002, Ferm *et al.* 2005, 2006). Because temperature growth provokes an increase in biogenic VOC emissions and moist soil emits more $NO_X$ precursors in comparison with dry soil, atmospheric warming can increase ozone pollution near the ground.

In the boundary layer where ozone formation and destruction take place, the ozone state depends on a great number of dynamical processes, all strongly depending on meteorological parameters (solar radiation, height of the mixing layer, wind speed, temperature) (Chattopadhyay and Chattopadhyay 2009). These factors, to a considerable degree, complicate analysis of ozone variations. In addition, the strong interannual ozone variability masks the ozone trend and influences climate change (Racherla and Adams 2008). However, a detailed study of ozone behaviour observed under special conditions gives us an opportunity to identify the impact of individual processes on the atmospheric ozone state (Varotsos 2002, 2003, Kolev *et al.* 2005, Lee *et al.* 2006). In the last decade, numerous investigations (mainly model studies) of climate–chemistry interactions have been performed, with the need for observational data being noted (Varotsos 2002, 2003, Kolev *et al.* 2005, Lee *et al.* 2006, Cracknell and Varotsos 2007, Isaksen *et al.* 2009).

Investigations presented in this article are extensions of our previous observations of the atmospheric ozone over Bulgaria (Donev *et al.* 2002, Kolev *et al.* 2008). Analysis of surface ozone behaviour in the Sofia boundary layer was performed with respect to studying the interannual variability of ozone concentrations. Dynamical processes in the atmospheric boundary layer, such as the destruction of the stable layer in early morning hours and the development of the mixing layer, which strongly affects the ozone state near the ground, were analysed using remote-sensing techniques – aerosol light detection and ranging (LIDAR) and ceilometer–LIDAR. For tracking the total ozone content (TOC) for a long period, including recent years, we used total ozone mapping spectrometer (TOMS) and scanning imaging absorption spectrometer for atmospheric cartography (SCIAMACHY) data.

## 2. Description of sites and instruments

Observations of the surface ozone behaviour were performed at three sites in Sofia (42° 39′ N, 23° 23′ E, 591 m a.s.l.). Site 1 is located at the Astronomical Observatory, which is situated in Borisova Gradina Park, and is surrounded by rich vegetation. Site 2 is located in the urbanized area, 'Druzhba'. This site is administered by the government (www.sofia.bg/). Site 3 is situated inside the premises of the Institute of Electronics, Bulgarian Academy of Sciences, and has open terrain with relatively little vegetation cover. An arterial highway passes close to this site.

Surface ozone concentrations ($C$) at sites 1 and 2 were measured using an ultraviolet optical absorption photometer (TECO 49), manufactured by Thermo Environmental Instruments Inc., Franklin, MA, USA, which determines the ozone concentration by measuring the attenuation of light at wavelength 254 nm due to ozone absorption in the cell with ambient air. At site 1, a photometer model, TECO 49 (Thermo Environmental Instruments, Inc.), was used. Due to the inherent stability of the ultraviolet absorption technique, it could be considered that the error of ozone concentrations reported here is within ±5 ppbV. At site 1, monitoring

of the meteorological parameters – total solar radiation ($R$), wind speed ($V$) and direction – was carried out at 10 m height using a pyranometer (model SP1110, Skye, Skye Instruments, Powys, UK) and wind monitor (model 05103, YOUNG, Scientific Sales Inc., Lawrenceville, NJ, USA). Air temperature ($T$) and relative humidity ($H_R$) were measured at 2 m height with an HMP45C sensor manufactured by Vaisala Inc., Woburn, MA, USA. At site 3, surface ozone concentration was measured with a solid-state chemiluminescent ozone analyser, model 3-02P, developed at OPTEC Inc. (St Petersburg, Russia). In 2008, this model of ozone analyser was successfully verified at the Advanced Monitoring Systems Center, operated by Battelle in cooperation with the Environment Protection Agency's National Exposure Research Laboratory. The detection method is based on the fast reaction of ozone with a sensitive reagent that produces chemiluminescent radiation. The relative error of the presented measurements does not exceed 15%. The sampling was performed through Teflon tubing at a height of approximately 12 m above ground level.

Observations of the boundary layer structure and dynamics were made with remote-sensing techniques – ceilometer–LIDAR and aerosol LIDAR operated at sites 1 and 3, respectively. The commercial ceilometer CHM 15k was manufactured in Germany by Jenoptik Laser (Optik, Systeme GmbH) and has the following main characteristics: light source – a laser protection class 1M with wavelength 1064 nm, pulse duration about 1 ns, energy per pulse 8 μJ, pulse repetition rate 5–7 kHz and measuring range 30–15 000 m with a resolution of 15 m. The aerosol LIDAR produced by the Institute of Electronics, Bulgarian Academy of Sciences, has the following characteristics: light source – a standard Nd-YAG laser operating at wavelength 532 nm; pulse duration and energy are 15–20 ns and 10–15 mJ, respectively; and the repetition rate is 12.5 Hz (Kolev *et al.* 2004, 2007).

## 3. Results and discussion

### 3.1 *Surface ozone in the Sofia boundary layer*

Now, it is recognized that the synoptic circulation, which greatly varies from year to year, influences the surface ozone state and its interannual variations (Kondratyev and Varotsos 2001a,b, Tang *et al.* 2009). Taking into account that this influence is more strongly expressed during spring–summer time, when enhanced atmospheric dynamics and photochemical ozone formation take place, we performed the analysis of the interannual ozone variations in the more stable autumn period. To reduce the number of factors influencing ozone variability, experimental observations performed in recent years at close meteorological conditions were chosen for the analysis. Table 1 shows, for example, that at site 1 on 4 October 2007 and 1 October 2008, meteorological conditions were similar – the measured values of the solar radiation intensity, temperature, relative humidity and wind speed were very close. Figure 1 shows diurnal variations of the solar radiation and temperature measured on these dates. At site 2, a similar situation was observed on 13 October 2008 and 8 October 2009. The measurements of the solar radiation intensity and temperature on these days are presented in figure 2.

In both cases, anticyclonic conditions ensured fine weather, which is favourable for photochemical ozone production. The analysis of the solar radiation behaviour presented in figures 1 and 2 shows that, for every site, the diurnal radiation variations

Table 1. Comparison of the values of meteorological parameters (intensity of solar radiation, temperature, relative humidity, wind speed) and surface ozone concentrations measured at site 1 in Sofia on 4 October 2007 and 1 October 2008.

| | $R$ (W m$^{-2}$) | | $T$ (°C) | | $H_R$ (%) | | $V$ (m s$^{-1}$) | | $C$ (ppbV) | |
|---|---|---|---|---|---|---|---|---|---|---|
| h | 2007 | 2008 | 2007 | 2008 | 2007 | 2008 | 2007 | 2008 | 2007 | 2008 |
| 8:00 | 93 | 92 | 6.6 | 5.3 | 97.6 | 96.4 | 0 | 0.1 | 2.4 | 1.9 |
| 9:00 | 275 | 282 | 8.4 | 7.0 | 97.2 | 96.0 | 0.1 | 0.15 | 2.4 | 1.9 |
| 10:00 | 441 | 454 | 11.0 | 9.9 | 81.1 | 78.3 | 0.2 | 0.3 | 2.9 | 3.0 |
| 11:00 | 572 | 556 | 13.9 | 12.3 | 70.3 | 67.8 | 0.25 | 0.4 | 4.1 | 11.4 |
| 12:00 | 625 | 567 | 16.7 | 14.8 | 58.8 | 60.7 | 0.2 | 0.3 | 12.4 | 10.5 |
| 13:00 | 673 | 692 | 18.9 | 16.6 | 48.8 | 53.4 | 0.3 | 0.4 | 23.0 | 20.2 |
| 14:00 | 609 | 679 | 20.5 | 18.5 | 43.2 | 46.6 | 0.3 | 0.5 | 30.0 | 32.1 |
| 15:00 | 523 | 565 | 21.4 | 19.7 | 38.7 | 41.7 | 0.35 | 0.6 | 33.5 | 35.8 |
| 16:00 | 400 | 437 | 21.7 | 20.3 | 36.3 | 41.8 | 0.3 | 0.5 | 34.5 | 35.5 |
| 17:00 | 234 | 242 | 20.0 | 18.7 | 49.2 | 48.0 | 0.2 | 0.4 | 18.7 | 32.6 |
| 18:00 | 35 | 51 | 17.7 | 17.9 | 61.3 | 52.5 | 0.3 | 0.3 | 1.8 | 26.3 |
| 19:00 | 1 | 2 | 15.5 | 15.9 | 69.6 | 62.1 | 0.4 | 0.3 | 2.1 | 12.9 |



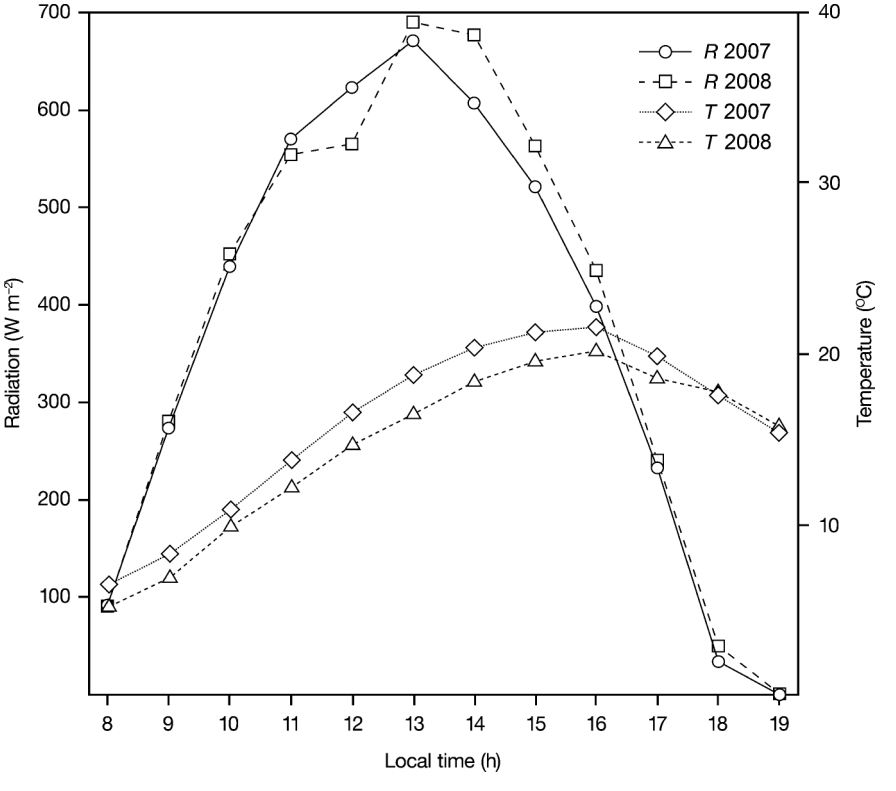


Figure 1. Diurnal variations of solar radiation and temperature measured at site 1 on 4 October 2007 and 1 October 2008.

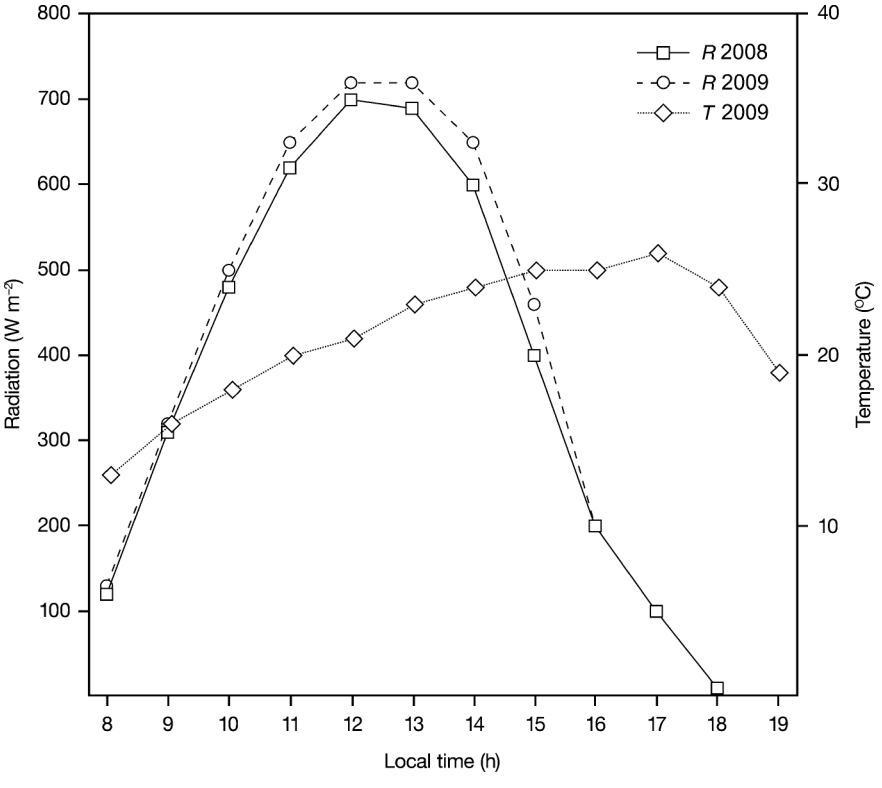


Figure 2. Diurnal variations of solar radiation measured at site 2 on 13 October 2008 and 8 October 2009. Temperature was measured on 8 October 2009.

practically do not vary from year to year, but each site demonstrates its own form of radiation behaviour. The maximum values of air temperature at both sites demonstrate time delay (about 3 h) relative to those of the solar radiation. The time series of surface ozone concentrations are shown in figures 3 and 4.

The features of the diurnal surface ozone variations are typical for urban sites with ozone maximum during daytime and minimum during evening and night hours. It should be pointed out that, as shown in figures 3 and 4, ozone demonstrates a striking resemblance in its interannual behaviour at both sites, particularly from early morning to afternoon. In morning hours, the increasing solar radiation starts up two processes, which increase ozone concentrations near the ground. The first is the development of the boundary layer caused by heating of the ground surface and the second is the creation of turbulent transfer of warm air to the higher atmospheric layers. This provides the development of the convective mixing layer and the destruction of the residual layer, in which the anthropogenic ozone formed in previous days could be accumulated, followed by the vertical transport of the ozone-rich air from aloft to the ground. The second process is the photochemical ozone formation from ozone precursors $NO_X$ and VOC with anthropogenic and biogenic origin. Briefly, the scheme of the photochemical $O_3$ formation may be described by a chain of the following reactions:

$$NO_2 + h\nu \rightarrow NO + O\left(^3P\right), \qquad \lambda \leq 400\,\text{nm}, \tag{1}$$

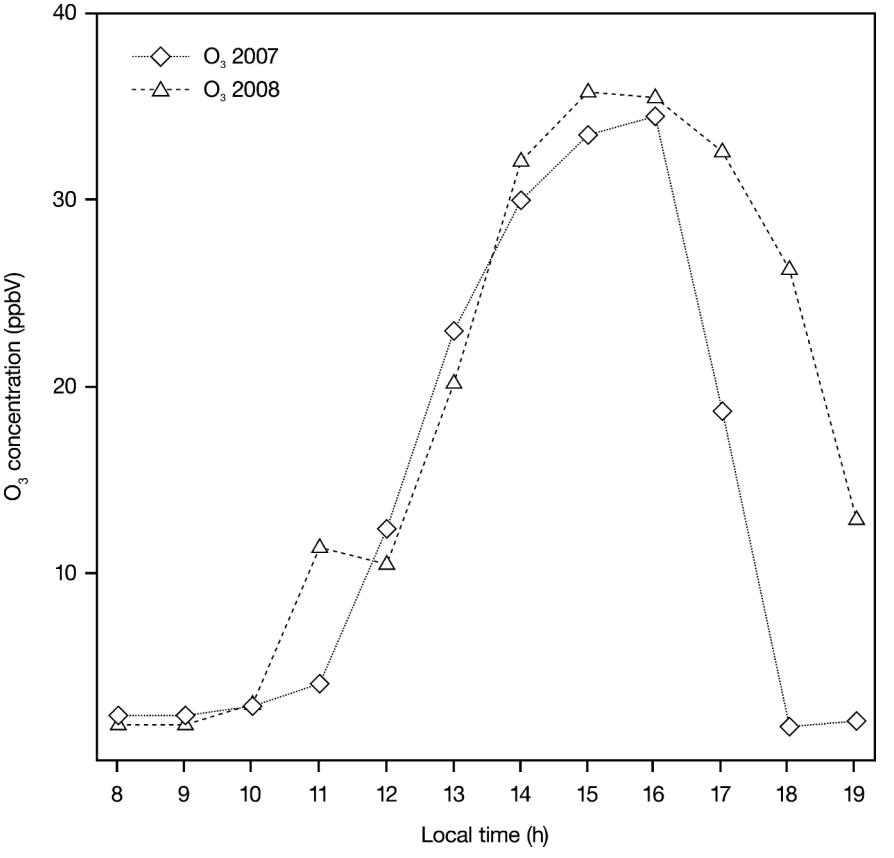


Figure 3. Diurnal variations of the surface ozone concentrations measured at site 1 on 4 October 2007 and 1 October 2008.

$$O_2 + O\left(^3P\right) + M \rightarrow O_3 + M, \tag{2}$$

$$NO + O_3 \rightarrow NO_2 + O_2, \tag{3}$$

where M is a random air molecule ($N_2$ or $O_2$), *hv* is the symbol for photon, which is an elementary particle, the quantum of the electromagnetic interaction and basic unit of light. In equations (1) and (7), the *hv* symbol shows that reactions, described by equations (1) and (7), are photochemical reactions. The stationary state of this system can be shifted to increasing ozone by peroxy radicals, $RO_2$, which can convert NO into $NO_2$:

$$NO + RO_2 \rightarrow NO_2 + RO. \tag{4}$$

In the boundary layer, $RO_2$ radicals are performed as a result of VOC oxidation by OH radicals:

$$H_{RH} + OH \rightarrow R + H_2O, \tag{5}$$

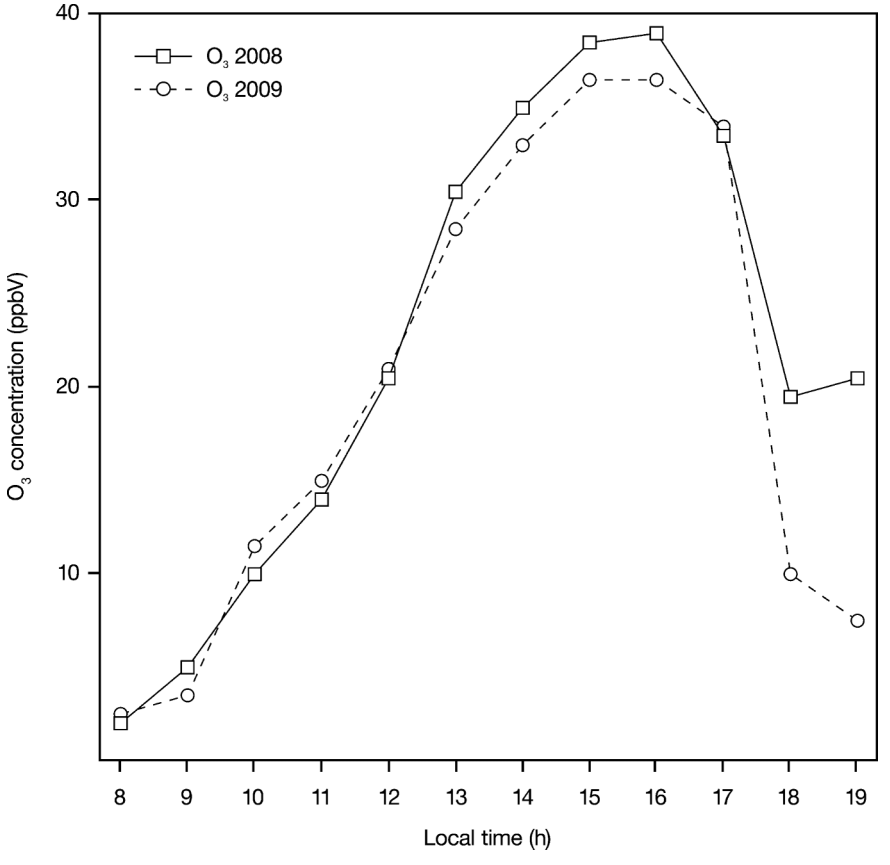


Figure 4. Diurnal variations of the surface ozone concentrations measured at site 2 on 13 October 2008 and 8 October 2009.

$$R + O_2 + M \rightarrow RO_2 + M. \tag{6}$$

OH radicals are produced primarily by the photolysis of ozone, with their concentration in atmosphere being defined by the concentration of water vapour:

$$O_3 + h\nu \rightarrow O\left(^1D\right) + O_2, \quad \lambda \leq 310\,\text{nm}, \tag{7}$$

$$O\left(^1D\right) + H_2O \rightarrow 2OH. \tag{8}$$

Taking into account that the efficiency of the reactions (1)–(8) strongly depends on the $VOC/NO_X$ ratio, which, in many cases, is different in various points over large urban areas, different levels of ozone concentrations can be detected at the monitoring sites. In the evening, under developing nocturnal inversion, when processes generating ozone are absent, the fast decrease of ozone near the ground is caused by $O_3$ destruction due to dry deposition (on Earth's ground and aerosols) and ozone titration with nitric oxide in accordance with reaction (3). The ozone state becomes very sensitive

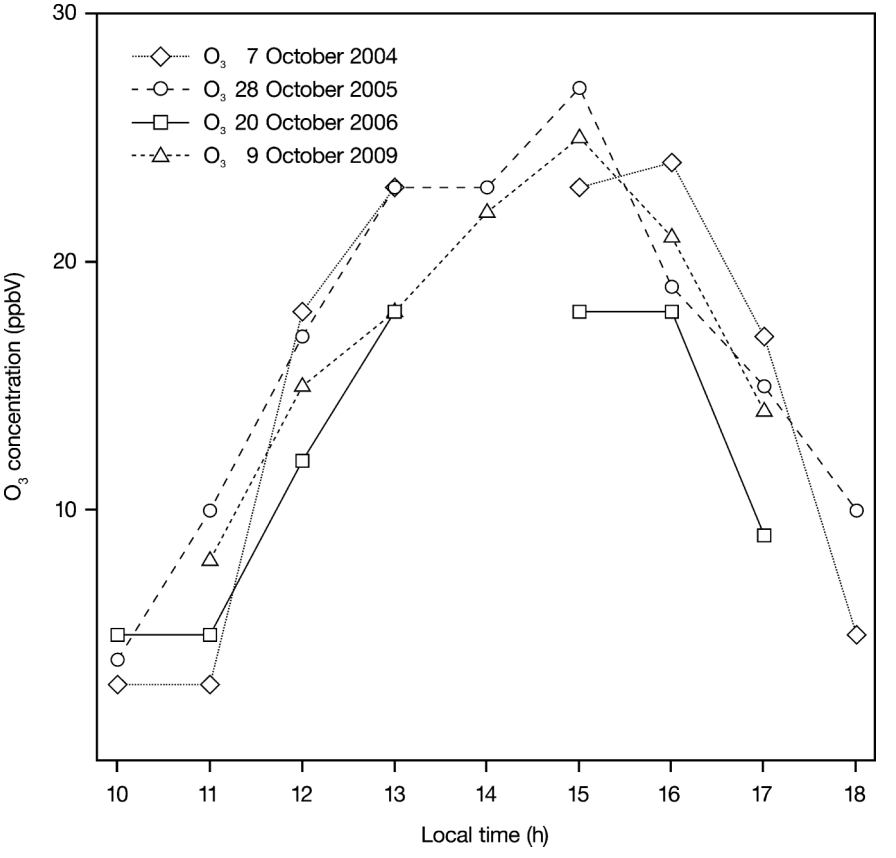


Figure 5. Interannual variations of the surface ozone concentrations measured at site 3 in October 2004, 2005, 2006 and 2009.

to wind, which creates horizontal advection, and the generating turbulence creates vertical mixing (figures 3 and 4).

Comparison of the time series of the surface ozone concentrations detected at site 3 during some days in October 2004, 2005, 2006 and 2009 is shown in figure 5.

Observations have been mainly performed at anticyclonal conditions on cloudless days with low wind speed, but the meteorological parameters (solar radiation, temperature) were not exactly the same. On the whole, ozone data received in different years demonstrate a good recurrence (the relative accuracy of the measurements was 15%). The lower values of maximum ozone concentrations, which were detected at site 3, in comparison with those at sites 1 and 2, can be attributed to its location near the highway. Vehicle exhausts change the $VOC/NO_X$ ratio and processes (1)–(8) of photochemical ozone formation.

Analysis of the presented observations shows the following.

1. In spite of the great temporal variability (including interannual), which the surface ozone demonstrates in the general case, in autumn, during anticyclonal cloudless weather and at close meteorological conditions (intensity of solar

radiation, temperature), the diurnal ozone variations (increase in $O_3$ concentrations during the development of the mixing layer, maximum values and time of its appearance – figures 3–5) show stable behaviour from year to year. So, it can be assumed that the boundary layer and ozone precursor concentrations, which are involved in photochemical ozone formation in accordance with reactions (1)–(8), keep up their state from year to year at the mentioned conditions. This fact can be used when temporal ozone trend and climate change influence on ozone are investigated.

2. Discrepancy in the form of ozone increasing from early morning to afternoon at sites 1–3 is observed in figures 3–5, respectively. It reflects the difference in the boundary layer development caused by the difference in the properties of the underlying surfaces at sites 1 and 2. At site 1, which is situated in a park zone, a great part of the incoming solar radiation is spent on the evaporation of moisture from vegetation and soil. For this reason, the development of the mixing layer (and increase in ozone concentrations) occurs with delay in relation to that at site 2, which is located in a more urbanized area surrounded by buildings.
3. Although the efficiency of the two basic reactions (1) and (7) in the chain of reactions (1)–(8), forming anthropogenic ozone, strongly depends on the intensity of the solar radiation, ozone behaviour at sites 1 and 2 shows direct correlation with the temperature (figures 1–4), which directly does not take part in these reactions. Additional analysis is needed to receive more detailed information about processes that determined the ozone state during observations.
4. Observations of the dynamics of the boundary layer, which influences the ozone state, have been performed at site 3 with aerosol LIDAR for many years (Kolev *et al.* 2004, 2008). An example of such observations performed in the autumn period at anticyclonal conditions is presented in figure 6. LIDAR data registered on 17 October 2006 show that the mixing layer started to form after 08:50 h. The mixing layer height ($H$) gradually increased until 11:30 h, reaching $H = 400$–$450$ m. After this time, a rapid growth of the mixing layer height is seen and its height reached $H = 1200$–$1400$ m at 13:30 h. In this case, a gradual growth of ozone concentration is also observed. Ceilometer observations at site 1 have been performed since May 2009. Experimental data (figure 7) obtained on 10 October 2009 demonstrate a complex boundary layer structure with two parts of the residual layer. The first part is observed at height $H = 800$ m and the second at height $H = 1250$ m. These layers were fully destroyed after 12:00 h. The mixing layer reached its maximum height, approximately $H = 2100$ m, at about 15:30 h. The joint interpretation of the mixing layer height data, mixing layer development and surface ozone concentration data can be summarized as follows: the surface ozone concentration varies in a manner similar to the mixing layer development in the three regions of observations. The maximum values of the surface ozone concentration at site 3 are reached 1–2 h after the mixing layer is fully developed. In the region of the Astronomical Observatory (site 1), the maximum values of the mixing layer height and surface ozone concentration were detected at approximately the same time.

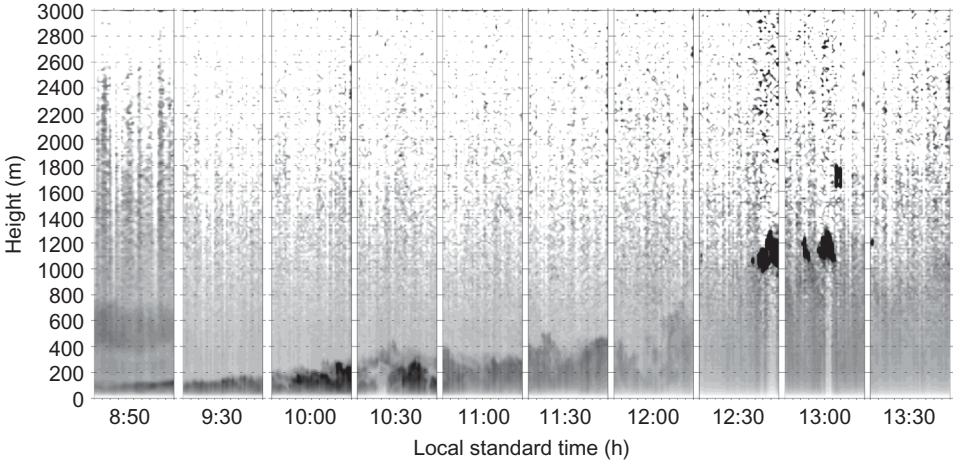


Figure 6. Height–time indicators constructed from LIDAR data obtained on 17 October 2006.

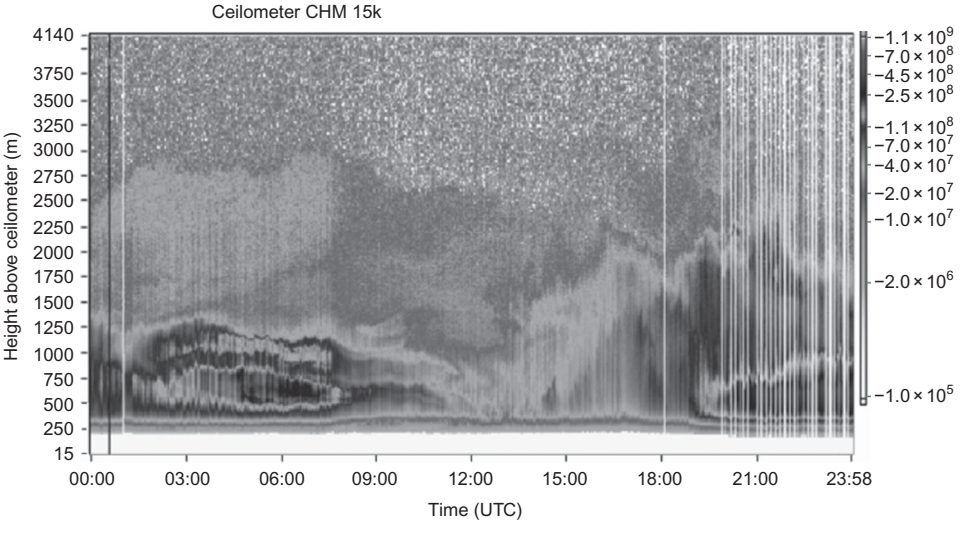


Figure 7. Height–time indicators constructed from ceilometer data obtained on 10 October 2009.

### 3.2 *Total ozone content*

Long-term (1997–2008) TOC variations over the Sofia region were analysed. The TOMS (1997–2002) and SCIAMACHY (2003–2008) total ozone monthly mean data were used. The TOC results from both instruments simultaneously operating in the period 2002–2005 were compared (figure 8). Good agreement between the data (correlation coefficient $r = 0.95$) was obtained. This fact allows us to use the TOMS data (1997–2002) and the SCIAMACHY data (2003–2008) sequentially for investigation of the total ozone behaviour in the period 1997–2008 (figure 9). Along with the seasonal TOC variations, quasi-biennial periodicity in the amplitude of the ozone maximum is seen. In 2003, 2005 and 2007, these amplitudes are higher than in 2002, 2004, 2006

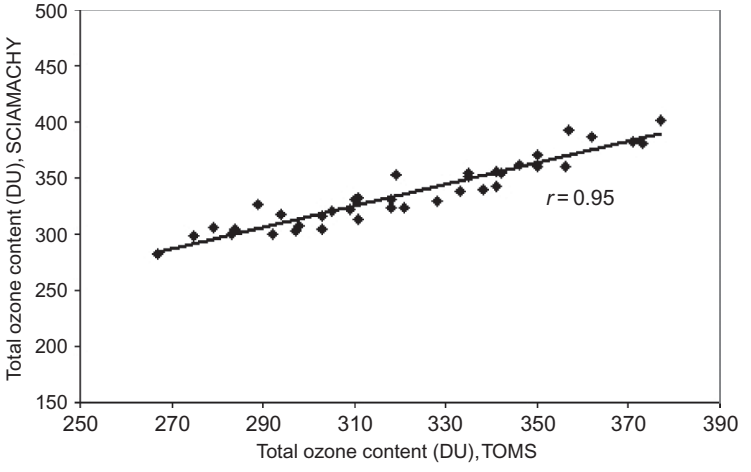


Figure 8. Correlation of TOC monthly mean values measured by TOMS and SCIAMACHY in 2002–2005.

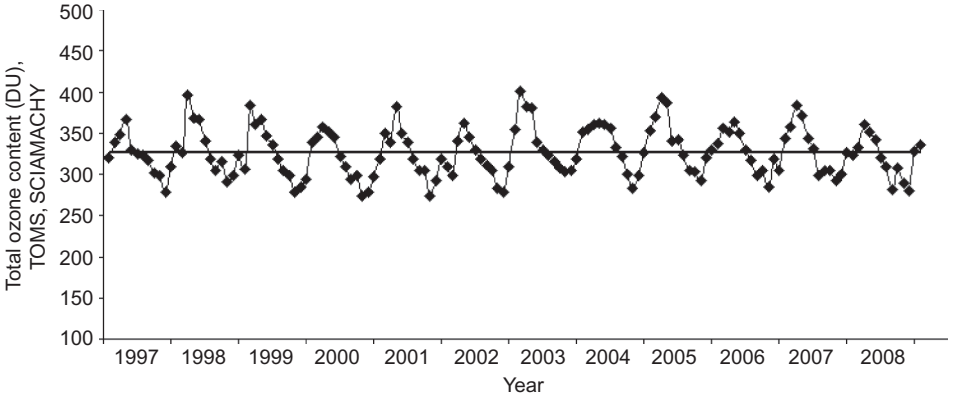


Figure 9. Interannual variations of the TOC monthly mean values received from TOMS (1997–2002) and SCIAMACHY (2003–2008) data.

and 2008. The highest TOC maximum (about 400 DU) was registered in March 2003. This fact may be interesting with respect to the situation that took place over Europe in 2003 during the so-called heatwave, when extremely high surface ozone concentrations were measured. Analysis of the long-term TOC variations did not find a total ozone trend in the period 1997–2008.

## 4. Conclusion

Surface ozone variations in the Sofia region in recent years have been studied with ozonometers, aerosol LIDAR and ceilometers. Analysis of the surface ozone and boundary layer observations performed at three monitoring sites found that, at close meteorological conditions in the autumn period, boundary layer development and diurnal ozone variations (ozone dynamics from morning hours to afternoon, maximum values) show similar behaviour from year to year during the analysed period.

These findings can be useful when surface ozone trend and climate change effects are investigated. There seems to be no significant trend in the total ozone over Sofia during the period 1997–2008.

**Acknowledgement**

Investigations were performed within the frame of the contract: 'City versus Mountain Tropospheric Ozone: The Sofia-Plana Region in an Air Quality and Ecological Sustainability Perspective' (contract DO 02-127/08).



**References**

Bandyopadhyay, G. and Chattopadhyay, S., 2007, Single hidden layer artificial neural network models versus multiple linear regression model in forecasting the time series of total ozone. *International Journal of Environmental Science and Technology*, **4**, pp. 141–149.

Cartalis, C. and Varotsos, C., 1994, Surface ozone in Athens, Greece, at the beginning and at the end of the 20th-century. *Atmospheric Environment*, **28**, pp. 3–8.

Chandra, S. and Varotsos, C.A., 1995, Recent trends of the total column ozone: implications for the Mediterranean region. *International Journal of Remote Sensing*, **16**, pp. 1765–1769.

Chattopadhyay, G. and Chattopadhyay, S., 2009, Predicting daily total ozone over Kolkata, India: skill assessment of different neural network models. *Meteorological Applications*, **16**, pp. 179–190.

Chattopadhyay, S. and Bandyopadhyay, G., 2007, Artificial neural network with back-propagation learning to predict mean monthly total ozone in Arosa, Switzerland. *International Journal of Remote Sensing*, **28**, pp. 4471–4482.

Cracknell, A.P. and Varotsos, C.A., 2007, The IPCC Fourth Assessment Report and the fiftieth anniversary of Sputnik. *Environmental Science and Pollution Research*, **14**, pp. 384–387.

Donev, E., Zeller, K. and Avramov, A., 2002, Preliminary background ozone concentrations in the mountain and coastal areas of Bulgaria. *Environmental Pollution*, **117**, pp. 281–286.

Efstathiou, M., Varotsos, C. and Kondratyev, K.Y., 1998, An estimation of the surface ultraviolet irradiance during an extreme total ozone minimum. *Meteorology and Atmospheric Physics*, **68**, pp. 171–176.

Efstathiou, M.N., Varotsos, C.A., Singh, R.P., Cracknell, A.P. and Tzanis, C., 2003, On the longitude dependence of total ozone trends over middle latitudes. *International Journal of Remote Sensing*, **24**, pp. 1361–1367.

Ferm, M., De Santis, F. and Varotsos, C., 2005, Nitric acid measurements in connection with corrosion studies. *Atmospheric Environment*, **39**, pp. 6664–6672.

Ferm, M., Watt, J., O'Hanlon, S., De Santis, F. and Varotsos, C., 2006, Deposition measurement of particulate matter in connection with corrosion studies. *Analytical and Bioanalytical Chemistry*, **384**, pp. 1320–1330.

Gernandt, H., Goersdorf, U., Claude, H. and Varotsos, C.A., 1995, Possible impact of polar stratospheric processes on mid-latitude vertical ozone distributions. *International Journal of Remote Sensing*, **16**, pp. 1839–1850.

Isaksen, I.S.A., Granier, C., Myhre, G., Berntsen, T.K., Dalsoren, S.B., Gauss, M., Klimont, Z., Benestad, R., Bousquet, P., Collins, W., Cox, T., Eyring, V., Fowler, D., Fuzzi, S., Joockel, P., Laj, P., Lohmann, U., Maione, M., Monks, P., Prevot, A.S.H., Raes, F., Richter, A., Rognerud, B., Schulz, M., Shindell, D., Stevenson, D.S., Storelvmo, T., Wang, W.C., van Weele, M., Wild, M. and

Wuebbles, D., 2009, Atmospheric composition change: climate–chemistry interactions. *Atmospheric Environment*, **43**, pp. 5138–5192.

Jacovides, C.P., Varotsos, C., Kaltsounides, N.A., Petrakis, M. and Lalas, D.P., 1994, Atmospheric turbidity parameters in the highly polluted site of Athens basin. *Renewable Energy*, **4**, pp. 465–470.

Kolev, N., Grigorov, I., Kolev, I., Devara, P.C.S., Raj, P.E. and Dani, K.K., 2007, Lidar-sunphotometer observations of atmospheric boundary layer characteristics over an urban area. *Boundary-Layer Meteorology*, **124**, pp. 99–115.

Kolev, N., Savov, P., Kaprielov, B., Grigorieva, V. and Kolev, I., 2008, The influence of the boundary layer development on the ozone concentration over urban area. *International Journal of Remote Sensing*, **29**, pp. 1877–1902.

Kolev, N., Tatarov, B., Grigorieva, V., Donev, E., Simeonov, P., Umlensky, V., Kaprielov, B. and Kolev, I., 2005, Aerosol lidar and *in-situ* ozone observations of the planetary boundary layer over Bulgaria during the solar eclipse of 11 August 1999. *International Journal of Remote Sensing*, **26**, pp. 3567–3584.

Kolev, N., Tatarov, B., Kaprielov, B. and Kolev, I., 2004, Investigation of the aerosol structure over an urban area using a polarization lidar. *Journal of Environmental Monitoring*, **19**, pp. 834–840.

Kondratyev, K.Y., Pokrovsky, O.M. and Varotsos, C.A., 1995, Atmospheric ozone trends and other factors of surface ultraviolet radiation variability. *Environmental Conservation*, **22**, pp. 259–261.

Kondratyev, K.Y. and Varotsos, C.A., 1995a, Atmospheric greenhouse effect in the context of global climate change. *Nuovo Cimento Della Societa Italiana Di Fisica C-Geophysics and Space Physics*, **18**, pp. 123–151.

Kondratyev, K.Y. and Varotsos, C.A., 1995b, Atmospheric ozone variability in the context of global change. *International Journal of Remote Sensing*, **16**, pp. 1851–1881.

Kondratyev, K.Y. and Varotsos, C.A., 1996, Global total ozone dynamics – impact on surface solar ultraviolet radiation variability and ecosystems. 1. Global ozone dynamics and environmental safety. *Environmental Science and Pollution Research*, **3**, pp. 153–157.

Kondratyev, K.Y. and Varotsos, C.A., 2001a, Global tropospheric ozone dynamics – part I: tropospheric ozone precursors. *Environmental Science and Pollution Research*, **8**, pp. 57–62.

Kondratyev, K.Y. and Varotsos, C.A., 2001b, Global tropospheric ozone dynamics – part II: numerical modeling of tropospheric ozone variability. *Environmental Science and Pollution Research*, **8**, pp. 113–119.

Kondratyev, K.Y. and Varotsos, C.A., 2002, Remote sensing and global tropospheric ozone observed dynamics. *International Journal of Remote Sensing*, **23**, pp. 159–178.

Kondratyev, K.Y., Varotsos, C.A. and Cracknell, A.P., 1994, Total ozone amount trend at St-Petersburg as deduced from NIMBUS-7 TOMS observations. *International Journal of Remote Sensing*, **15**, pp. 2669–2677.

Lee, J.D., Lewis, A.C., Monks, P.S., Jacob, M., Hamilton, J.F., Hopkins, J.R., Watson, N.M., Saxton, J.E., Ennis, C., Carpenter, L.J., Carslaw, N., Fleming, Z., Bandy, B.J., Oram, D.E., Penkett, S.A., Slemr, J., Norton, E., Rickard, A.R., Whalley, L.K., Heard, D.E., Bloss, W.J., Gravestock, T., Smith, S.C., Stanton, J., Pilling, M.J. and Jenkin, M.E., 2006, Ozone photochemistry and elevated isoprene during the UK heatwave of August 2003. *Atmospheric Environment*, **40**, pp. 7598–7613.

Racherla, P.N. and Adams, P.J., 2008, The response of surface ozone to climate change over the Eastern United States. *Atmospheric Chemistry and Physics*, **8**, pp. 871–885.

Reid, S.J., Rex, M., Von Den Gathen, P., Floisand, I., Stordal, F., Carver, G.D., Beck, A., Reimer, E., Kruger-Cartensen, R., De Haan, L.L., Braathen, G., Dorokhov, V., Fast, H., Kyri, E., Gil, M., Litynska, Z., Molyneux, M., Murphy, G., O'connor, F., Ravengani, F., Varotsos, C., Wenger, J. and Zerefos, C., 1998,

A study of ozone laminae using diabatic trajectories, contour advection and photochemical trajectory model simulations. *Journal of Atmospheric Chemistry*, **30**, pp. 187–207.

Reid, S.J., Vaughan, G., Mitchell, N.J., Prichard, I.T., Smit, H.J., Jorgensen, T.S., Varotsos, C. and De Backer, H., 1994, Distribution of the ozone laminae during EASOE and the possible influence of inertia-gravity waves. *Geophysical Research Letters*, **21**, pp. 1479–1482.

Schulz, A., Rex, M., Harris, N.R.P., Braathen, G.O., Reimer, E., Alfier, R., Kilbane-Dawe, I., Eckermann, S., Allaart, M., Alpers, M., Bojkov, B., Cisneros, J., Claude, H., Cuevas, E., Davies, J., De Backer, H., Dier, H., Dorokhov, V., Fast, H., Godin, S., Johnson, B., Kois, B., Kondo, Y., Kosmidis, E., Kyro, E., Litynska, Z., Mikkelsen, I.S., Molyneux, M.J., Murphy, G., Nagai, T., Nakane, H., O'connor, F., Parrondo, C., Schmidlin, F.J., Skrivankova, P., Varotsos, C., Vialle, C., Viatte, P., Yushkov, V., Zerefos, C. and Von Der Gathen, P., 2001, Arctic ozone loss in threshold conditions: match observations in 1997/1998 and 1998/1999. *Journal of Geophysical Research*, **106**, pp. 7495–7503.

Schulz, A., Rex, M., Steger, J., Harris, N.R.P., Braathen, G.O., Reimer, E., Alfier, R., Beck, A., Alpers, M., Cisneros, J., Claude, H., De Backer, H., Dier, H., Dorokhov, V., Fast, H., Godin, S., Hansen, G., Kanzawa, H., Kois, B., Kondo, Y., Kosmidis, E., Kyro, E., Litynska, Z., Molyneux, M.J., Murphy, G., Nakane, H., Parrondo, C., Ravegnani, F., Varotsos, C., Vialle, C., Viatte, P., Yushkov, V., Zerefos, C. and Von Der Gathen, P., 2000, Match observations in the Arctic winter 1996/97: high stratospheric ozone loss rates correlate with low temperatures deep inside the polar vortex. *Geophysical Research Letters*, **27**, pp. 205–208.

Tang, L., Chen, D., Karlsson, P.E., Gu, Y. and Ou, T., 2009, Sinoptic circulation and its influence on spring and summer surface ozone concentrations in southern Sweden. *Boreal Environment Research*, **14**, pp. 889–902.

Varotsos, C., 1994, Solar ultraviolet radiation and total ozone, as derived from satellite and ground-based instrumentation. *Geophysical Research Letters*, **21**, pp. 1787–1790.

Varotsos, C., 2002, The southern hemisphere ozone hole split in 2002. *Environmental Science and Pollution Research*, **9**, pp. 375–376.

Varotsos, C., 2003, What is the lesson from the unprecedented event over Antarctica in 2002? *Environmental Science and Pollution Research*, **10**, pp. 80–81.

Varotsos, C., Alexandris, D., Chronopoulos, G. and Tzanis, C., 2001a, Aircraft observations of the solar ultraviolet irradiance throughout the troposphere. *Journal of Geophysical Research-Atmospheres*, **106**, pp. 14843–14854.

Varotsos, C., Cartalis, C., Vlamakis, A., Tzanis, C. and Keramitsoglou, I., 2004, The long-term coupling between column ozone and tropopause properties. *Journal of Climate*, **17**, pp. 3843–3854.

Varotsos, C., Kondratyev, K.Y. and Efstathiou, M., 2001b, On the seasonal variation of the surface ozone in Athens, Greece. *Atmospheric Environment*, **35**, pp. 315–320.

Varotsos, C., Kondratyev, K.Y. and Katsikis, S., 1995, On the relationship between total ozone and solar ultraviolet radiation at St Petersburg, Russia. *Geophysical Research Letters*, **22**, pp. 3481–3484.

Varotsos, C.A. and Cracknell, A.P., 1993, Ozone depletion over Greece as deduced from Nimbus-7 TOMS measurements. *International Journal of Remote Sensing*, **14**, pp. 2053–2059.

Varotsos, C.A. and Cracknell, A.P., 1994, Three years of total ozone measurements over Athens obtained using the remote sensing technique of a Dobson spectrophotometer. *International Journal of Remote Sensing*, **15**, pp. 1519–1524.

Varotsos, C.A. and Cracknell, A.P., 2004, New features observed in the 11- year solar cycle. *International Journal of Remote Sensing*, **25**, pp. 2141–2157.

VAROTSOS, C.A., KONDRATYEV, K.Y. and CRACKNELL, A.P., 2000, New evidence for ozone depletion over Athens, Greece. *International Journal of Remote Sensing*, **21**, pp. 2951–2955.

ZIEMKE, J.R., CHANDRA, S., HERMAN, J. and VAROTSOS, C., 2000, Erythemally weighted UV trends over northern latitudes derived from Nimbus-7 TOMS measurements. *Journal of Geophysical Research-Atmospheres*, **105**, pp. 7373–7382.